5504 *Biochemistry* **2010,** *49,* 5504–5510
DOI: 10.1021/bi100433x

BIOCHEMISTRY
including biophysical chemistry & molecular biology
Article

Kinetic Basis of Nucleotide Selection Employed by a Protein Template-Dependent DNA Polymerase[†]

Jessica A. Brown,[‡,§] Jason D. Fowler,[‡] and Zucai Suo*[,‡,§,∥,⊥,@]

[‡]*Department of Biochemistry,* [§]*Ohio State Biochemistry Program,* [∥]*Ohio State Biophysics Program,* [⊥]*Molecular, Cellular and Developmental Biology Program, and* [@]*Comprehensive Cancer Center, The Ohio State University, Columbus, Ohio 43210*

Received March 23, 2010; Revised Manuscript Received May 5, 2010

ABSTRACT: Rev1, a Y-family DNA polymerase, contributes to spontaneous and DNA damage-induced mutagenic events. In this paper, we have employed pre-steady-state kinetic methodology to establish a kinetic basis for nucleotide selection by human Rev1, a unique nucleotidyl transferase that uses a protein template-directed mechanism to preferentially instruct dCTP incorporation. This work demonstrated that the high incorporation efficiency of dCTP is dependent on both substrates: an incoming dCTP and a templating base dG. The extremely low base substitution fidelity of human Rev1 (10^0 to 10^{-5}) was due to the preferred misincorporation of dCTP with templating bases dA, dT, and dC over correct dNTPs. Using non-natural nucleotide analogues, we showed that hydrogen bonding interactions between residue R357 of human Rev1 and an incoming dNTP are not essential for DNA synthesis. Lastly, human Rev1 discriminates between ribonucleotides and deoxyribonucleotides mainly by reducing the rate of incorporation, and the sugar selectivity of human Rev1 is sensitive to both the size and orientation of the 2′-substituent of a ribonucleotide.

The human genome encodes at least 16 DNA polymerases (Pol)[1] that are involved in replicating and maintaining the integrity of genomic DNA. Human DNA polymerases are classified into four families: A, B, X, and Y. Y-Family DNA polymerases are involved in DNA damage tolerance pathways, whereby a Y-family enzyme rescues stalled DNA replication at sites of DNA damage. Humans have four known Y-family members: Polη, Polι, Polκ, and Rev1. Rev1 is found in the genome of all eukaryotes (*1*) and is capable of functioning in both catalytic and structural roles. Composed of 1251 amino acids (*2*), human Rev1 (hRev1) is organized into a central catalytic domain that is flanked by an N-terminal BRCT domain and a C-terminus with two ubiquitin-binding motifs and a domain for polymerase interactions (*3*). As a scaffold protein, Rev1 interacts with proliferating cell nuclear antigen (PCNA) (*4*−*7*), ubiquitinated proteins (*5*, *6*), and DNA polymerases η, κ, ι, and ζ (*8*−*15*). These findings support a model, whereby Rev1 is involved in polymerase switching at sites of DNA damage (*16*−*18*). With regard to enzymatic activity, hRev1 preferentially inserts dCTP opposite a templating base dG (*2*, *19*−*22*); however, unlike other human DNA polymerases, this incorporation event proceeds in a protein template-directed manner rather than a DNA template-dependent manner with Watson−Crick base pairing (*23*). Instead, the incoming dCTP hydrogen bonds with R357, and the extrahelical template base dG is accommodated in a hydrophobic pocket while L358 rests in the conventional location of a templating base (Figure 1) (*23*).

Rev1 and Polζ are responsible for the majority of spontaneous and DNA damage-induced mutagenic events in yeast; early studies reveal similar findings in mammalian cell lines (*24*−*26*). In human tissues, the rev1 gene is ubiquitously expressed, but the highest level of expression is in human testis and ovary based on RT-PCR results (*2*, *8*, *19*). Furthermore, hRev1 has been observed at replication foci during both G1 and S phases following UV irradiation (*27*). However, it has also been reported that the protein levels of hRev1 are unaffected by UV irradiation or cell cycle progression (*28*). In addition to a role in translesion synthesis, Rev1 has been implicated in somatic hypermutation, and current data suggest the catalytic domain participates in the generation of C to G transversions (*29*, *30*). To improve our understanding of the enzymatic function of hRev1, we have performed pre-steady-state kinetic analysis on a truncated version of hRev1. Our studies established a kinetic basis for nucleotide selection by hRev1.

EXPERIMENTAL PROCEDURES

Materials. These chemicals were purchased from the following companies: [γ-^{32}P]ATP, MP Biomedicals; deoxyribonucleotide 5′-triphosphates, GE Healthcare; ribonucleotide 5′-triphosphates, MBI Fermentas; 2′-aracytidine 5′-triphosphate (araCTP), 2′-deoxy-2′,2′-difluorocytidine 5′-triphosphate (GemCTP), 2′-fluoro-2′-deoxycytidine 5′-triphosphate (2′-F-CTP), 2′-*O*-methylcytidine

[†]This work was supported by National Institutes of Health Grants GM079403 and ES009127 to Z.S. J.A.B. was supported by an American Heart Association Predoctoral Fellowship (Grant 0815382D) and an International PEO Scholar Award. J.D.F. was supported by a Postdoctoral Fellowship from a Pulmonary National Institutes of Health Training Grant 5T32HL007946 (principal investigator, Mark D. Wewers).

*To whom correspondence should be addressed: 880 Biological Sciences, 484 West 12th Ave., Columbus, OH 43210. Telephone: (614) 688-3706. Fax: (614) 292-6773. E-mail: suo.3@osu.edu.

[1]Abbreviations: 2′-F-CTP, 2′-fluoro-2′-deoxycytidine 5′-triphosphate; 2′-OCH$_3$-CTP, 2′-*O*-methylcytidine 5′-triphosphate; araCTP, 2′-aracytidine 5′-triphosphate; BSA, bovine serum albumin; dNITP, 5-nitroindole 5′-triphosphate; dNTP, 2′-deoxyribonucleotide 5′-triphosphate; dPTP, pyrene 5′-triphosphate; DTT, dithiothreitol; EDTA, ethylenediaminetetraacetic acid; GemCTP, 2′-deoxy-2′,2′-difluorocytidine 5′-triphosphate; HhH, helix−hairpin−helix; hRev1, human Rev1; PCNA, proliferating cell nuclear antigen; Pol, DNA polymerase; Polβ, DNA polymerase β; Polη, DNA polymerase η; Polι, DNA polymerase ι; Polκ, DNA polymerase κ; Polλ, DNA polymerase λ; rNTP, ribonucleotide 5′-triphosphate; yRev1, yeast Rev1.

 Published on Web 06/02/2010

5′-triphosphate (2′-OCH_3-CTP), and 5-nitroindole 5′-triphosphate (dNITP), TriLink Biotechnologies; Bio-Spin 6 columns, Bio-Rad Laboratories; OptiKinase, USB Corp.; synthetic oligodeoxyribonucleotides 21-mer, 5′-phosphorylated 19-mer, and 41-mers, Integrated DNA Technologies. Pyrene 5′-triphosphate (dPTP) was a generous gift from J.-S. Taylor (Washington University at St. Louis, St. Louis, MO).

Expression and Purification of hRev1. Expression plasmid pBAD-REV1S, a generous gift from K. Kamiya at Hiroshima University (Hiroshima, Japan), encoded a truncated version of human Rev1 (residues 341−829) (*31*). The expression and purification of truncated human Rev1 were performed as previously described (*19*).

DNA Substrates. Commercially synthesized oligomers listed in Table 1 were purified using polyacrylamide gel electrophoresis (*32*, *33*). The 21-mer primer was radiolabeled with [γ-^{32}P]-ATP and OptiKinase according to the manufacturer's protocol, and the unreacted [γ-^{32}P]ATP was subsequently removed via a Bio-Spin 6 column. The primer−template DNA substrates (*32*) and single-nucleotide gap DNA substrate (*33*) were annealed as described previously.

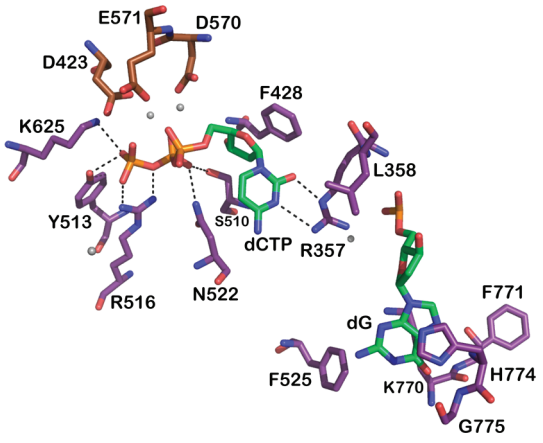

FIGURE 1: Active site of hRev1. Important active site residues that interact with an incoming dCTP or the templating base dG are shown (Protein Data Bank entry 3GQC). The dashed lines represent hydrogen bonds, and the four magnesium ions are shown as gray spheres.

Measurement of the k_p and K_d for Single-Nucleotide Incorporation. Kinetic assays were completed using buffer R [50 mM HEPES (pH 7.5 at 37 °C), 5 mM $MgCl_2$, 50 mM NaCl, 0.1 mM EDTA, 5 mM DTT, 10% glycerol, and 0.1 mg/mL BSA]. All kinetic experiments described here were performed at 37 °C, and the reported concentrations were final after all of the components had been mixed. A preincubated solution containing hRev1 (120 nM) and 5′-^{32}P-radiolabeled DNA substrate (30 nM) was mixed with increasing concentrations (0.2−800 μM) of nucleotide in buffer R at 37 °C. Aliquots of the reaction mixtures were quenched at various times using 0.37 M EDTA. A rapid chemical-quench flow apparatus (KinTek) was utilized for fast nucleotide incorporations. Reaction products were resolved using sequencing gel electrophoresis (17% acrylamide and 8 M urea) and quantitated with a Typhoon TRIO instrument (GE Healthcare). The time course of product formation at each nucleotide concentration was fit to a single-exponential equation (eq 1) using a nonlinear regression program, KaleidaGraph (Synergy Software), to yield an observed rate constant of nucleotide incorporation (k_{obs}). The k_{obs} values were then plotted as a function of nucleotide concentration and fit using the hyperbolic equation (eq 2) which resolved the k_p and K_d values for nucleotide incorporation catalyzed by hRev1.

$$[\text{product}] = A[1 - \exp(-k_{obs}t)] \quad (1)$$

$$k_{obs} = k_p[\text{dNTP}]/([\text{dNTP}] + K_d) \quad (2)$$

RESULTS

Kinetic Basis of dNTP Selection. Transient-state kinetic methods were employed to measure the substrate specificity and polymerase fidelity of a truncated form of hRev1. A preincubated solution of hRev1 (120 nM) and 5′-^{32}P-labeled D-G DNA (30 nM) was mixed with increasing concentrations of dCTP·Mg^{2+} (see Experimental Procedures). These single-turnover conditions in which hRev1 is in molar excess over DNA permit the direct observation of the DNA substrate being converted to the extended

Table 1: Sequences of the D-DNA Substrates[a]

D-G	5′-CGCAGCCGTCCAACCAACTCA-3′
	3′-GCGTCGGCAGGTTGGTTGAGT**G**TCAGCTAGGTTACGGCAGG-5′
D-A	5′-CGCAGCCGTCCAACCAACTCA-3′
	3′-GCGTCGGCAGGTTGGTTGAGT**A**TCAGCTAGGTTACGGCAGG-5′
D-T	5′-CGCAGCCGTCCAACCAACTCA-3′
	3′-GCGTCGGCAGGTTGGTTGAGT**T**TCAGCTAGGTTACGGCAGG-5′
D-C	5′-CGCAGCCGTCCAACCAACTCA-3′
	3′-GCGTCGGCAGGTTGGTTGAGT**C**TCAGCTAGGTTACGGCAGG-5′
D-G Gap	5′-CGCAGCCGTCCAACCAACTCA AGTCGATCCAATGCCGTCC-3′
	3′-GCGTCGGCAGGTTGGTTGAGT**G**TCAGCTAGGTTACGGCAGG-5′

[a]Each DNA substrate is composed of a 5′-radiolabeled 21-mer and a 41-mer template which has the unique template bases in bold. D-G Gap has a 5′-phosphorylated 19-mer.

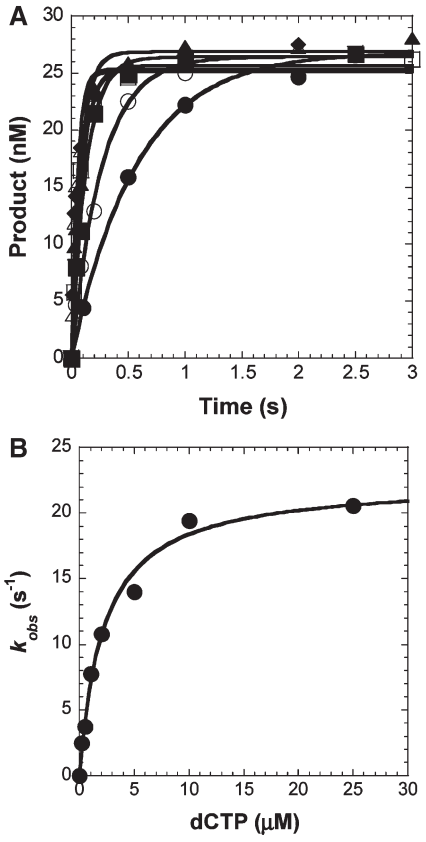

FIGURE 2: Concentration dependence of the pre-steady-state rate constant of deoxycytidyl transferase catalyzed by hRev1. (A) A preincubated solution of hRev1 (120 nM) and 5′-^{32}P-labeled D-6T (30 nM) was rapidly mixed for various time intervals with increasing concentrations of dCTP·Mg^{2+}: 0.2 (●), 0.5 (○), 1 (■), 2 (□), 5 (▲), 10 (△), and 25 μM (◆). The solid lines are the best fits to a single-exponential equation which determined the observed rate constant, k_{obs}. (B) k_{obs} values plotted as a function of dCTP concentration. The data (●) were then fit to a hyperbolic equation, yielding a k_p of 22.4 ± 0.9 s^{-1} and a K_d of 2.2 ± 0.3 μM.

DNA product in a single pass through the enzymatic pathway (*34*). The extended DNA product was quantitated, plotted (Figure 2), and fit to the appropriate equations (eq 1 or 2) that resolved a maximum rate of nucleotide incorporation (k_p) of 22.4 ± 0.9 s^{-1} and an equilibrium dissociation constant (K_d) of 2.2 ± 0.3 μM (Table 2). Notably, Tsai and Johnson report that nucleotide binding to T7 DNA polymerase, an A-family enzyme, induces several conformational changes preceding the incorporation step, thereby arguing that the measured K_d value under single-turnover reaction conditions is not a true equilibrium dissociation constant (*35*). Since there is no published evidence to support the existence of such conformational changes for the protein template-directed hRev1, we assume the K_d values measured in this paper reflect the true nucleotide binding affinity ($1/K_d$). To examine how efficiently hRev1 incorporates dCTP opposite other templating bases, we performed similar single-turnover assays using DNA substrates with dA (D-A), dC (D-C), and dT (D-T) as the template base (Table 2). The substrate specificity constants (k_p/K_d), efficiency ratio, and fidelity were calculated. The ground-state binding affinity decreased 4−55-fold, while the rate of dCTP incorporation was reduced by 7−12-fold when the templating base was not dG. Overall, the catalytic efficiency was up to 360-fold greater when dCTP was inserted into D-G. The preferential order of incorporation of dCTP opposite the four template bases was as follows: dG ≫ dA > dT ≈ dC.

Next, we measured the catalytic efficiency of nucleotide incorporation for the three remaining Watson−Crick base pair combinations under single-turnover conditions, and the kinetic data are listed in Table 2. Compared to that with the dCTP·dG base pair, the catalytic efficiency of hRev1 decreased 4900-, 12000-, and 42000-fold for the dTTP·dA, dATP·dT, and dGTP·dC base pairs, respectively. Despite a change in the identity of an incoming dNTP, the template preference remained the same on the basis of the substrate specificity constant as observed with dCTP. The binding affinity remained high for dATP but was ~14- and 20-fold weaker for dGTP and dTTP, respectively. Furthermore,

Table 2: Kinetic Parameters for the Incorporation of a Nucleotide into D-DNA Catalyzed by hRev1 at 37 °C

dNTP	k_p (s^{-1})	K_d (μM)	k_p/K_d (μM^{-1} s^{-1})	efficiency ratio[a]	fidelity[b]
			Template dG (D-G)		
dCTP	22.4 ± 0.9	2.2 ± 0.3	10		
dATP	0.050 ± 0.004	70 ± 20	7.1×10^{-4}	1.4×10^{4}	7.0×10^{-5}
dGTP	6.3 ± 0.3	90 ± 10	7.0×10^{-2}	1.5×10^{2}	6.8×10^{-3}
dTTP	0.88 ± 0.06	22 ± 7	4.0×10^{-2}	2.5×10^{2}	3.9×10^{-3}
			Template dA (D-A)		
dTTP	0.092 ± 0.007	44 ± 6	2.1×10^{-3}	4.9×10^{3}	
dCTP	1.87 ± 0.05	9.5 ± 0.8	2.0×10^{-1}	5.2×10	9.9×10^{-1}
			Template dT (D-T)		
dATP	0.00235 ± 0.00008	2.7 ± 0.4	8.7×10^{-4}	1.2×10^{4}	
dCTP	1.93 ± 0.05	35 ± 2	5.5×10^{-2}	1.8×10^{2}	9.8×10^{-1}
			Template dC (D-C)		
dGTP	0.0073 ± 0.0010	30 ± 10	2.4×10^{-4}	4.2×10^{4}	
dCTP	3.4 ± 0.2	120 ± 10	2.8×10^{-2}	3.6×10^{2}	9.9×10^{-1}
			Template dG (D-G Gap)		
dCTP	11 ± 1	8 ± 2	1.4	7.4	

[a]Calculated as $(k_p/K_d)_{dCTP\cdot D\text{-}G}/(k_p/K_d)_{dNTP\cdot dN}$. [b]Calculated as $(k_p/K_d)_{incorrect}/[(k_p/K_d)_{correct} + (k_p/K_d)_{incorrect}]$.

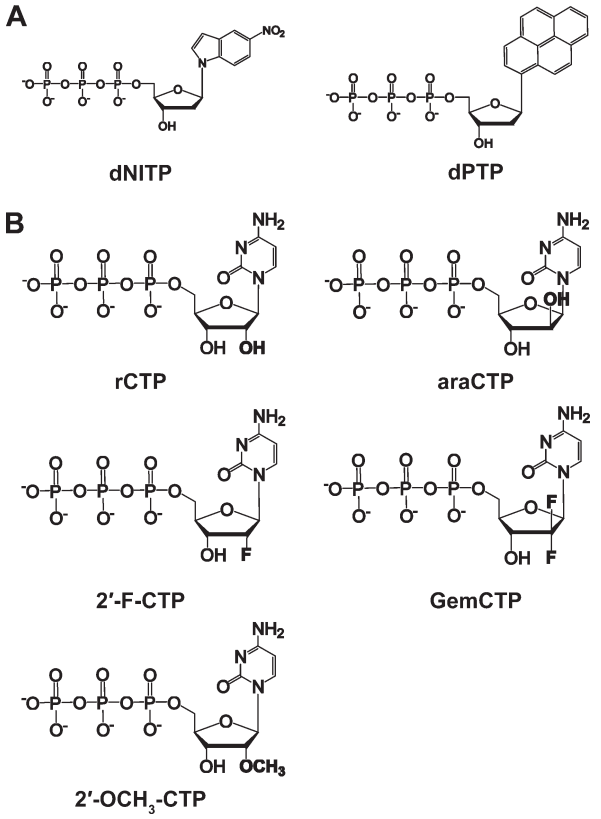

FIGURE 3: Chemical structures of nucleotide analogues: (A) non-natural nucleotide analogues and (B) CTP analogues used in this work.

the rate of incorporation of dCTP into D-A, D-T, and D-C DNA was up to 820-fold faster than the rate for canonical dNTP; therefore, the strong dCTP preference by hRev1 with templating bases dA, dT, and dC leads to an extremely low fidelity of ~1 (Table 2). Please note that enzyme fidelity is calculated using the standard kinetic equation, $(k_p/K_d)_{incorrect}/[(k_p/K_d)_{correct} + (k_p/K_d)_{incorrect}]$. When fidelity approaches a value of 1, this indicates that a misincorporation is favored over the canonical Watson−Crick base pair and that a correct incorporation is not likely to occur. Therefore, to improve our understanding of the frequency of a correct incorporation catalyzed by hRev1, the following equation was used: $(k_p/K_d)_{correct}/(k_p/K_d)_{dCTP\cdot dN}$. Here, the frequency of a correct incorporation is calculated to be 1.1×10^{-2}, 1.6×10^{-2}, and 8.6×10^{-3} for the dTTP·dA, dATP·dT, and dGTP·dC base pairs, respectively. These values translate into approximately one correct incorporation (dTTP, dATP, or dGTP) per 100 dCTP misincorporations.

Since hRev1 exhibited greater catalytic efficiency when dG is the template base, we determined the substrate specificity constant for the incorporation of the other dNTPs into D-G DNA (Table 2). The efficiency to form dATP·dG, dGTP·dG, and dTTP·dG base pairs was 1-, 290-, and 20-fold greater than those of dATP·dT, dGTP·dC, and dTTP·dA base pairs, respectively. Surprisingly, relative to the other template bases, the rate of nucleotide incorporation was up to 860-fold faster when the substrate had dG positioned as the template base. Meanwhile, the K_d value was at least 10-fold higher for addition of a non-dCTP into D-G DNA. The fidelity of hRev1 inserting dNTPs opposite dG ranged from 10^{-3} to 10^{-5}.

It has been shown that hRev1 may participate in cellular processes that involve gapped DNA (*36*). Determining the pre-steady-state kinetic parameters for dCTP incorporation into a single-nucleotide gapped DNA substrate (D-G Gap) revealed that hRev1 is 7-fold more efficient with the primer−template D-G DNA substrate (Table 2). This modest effect can be attributed to a 2-fold slower rate and a 4-fold weaker binding affinity for dCTP incorporation.

Table 3: Kinetic Parameters for Incorporation of Non-Natural Nucleotide Analogues into D-G DNA Catalyzed by hRev1 at 37 °C

dNTP	k_p (s^{-1})	K_d (μM)	k_p/K_d (μM^{-1} s^{-1})	efficiency ratio[a]
dCTP	22.4 ± 0.9	2.2 ± 0.3	10	
dATP	0.050 ± 0.004	70 ± 20	7.1×10^{-4}	1.4×10^{4}
dNITP	0.0457 ± 0.0006	15.8 ± 0.6	2.9×10^{-3}	3.5×10^{3}
dPTP	0.0228 ± 0.0008	25 ± 3	9.1×10^{-4}	1.1×10^{4}

[a]Calculated as $(k_p/K_d)_{dCTP}/(k_p/K_d)_{dNTP}$.

Table 4: Kinetic Parameters for Incorporation of CTP Analogues into D-G DNA Catalyzed by hRev1 at 37 °C

NTP	k_p (s^{-1})	K_d (μM)	k_p/K_d (μM^{-1} s^{-1})	sugar selectivity[a]
dCTP	22.4 ± 0.9	2.2 ± 0.3	10	
rCTP	0.098 ± 0.002	2.7 ± 0.2	3.6×10^{-2}	280
araCTP	6.3 ± 0.5	4 ± 1	1.6	6
2′-F-CTP	19.2 ± 0.5	3.5 ± 0.4	5.5	2
GemCTP	6.8 ± 0.4	29 ± 6	2.3×10^{-1}	43
2′-OCH_3-CTP	0.0122 ± 0.0006	8 ± 1	1.5×10^{-3}	6700

[a]Calculated as $(k_p/K_d)_{dCTP}/(k_p/K_d)_{analogue}$.

Importance of Hydrogen Bonding and Base Stacking. Crystallographic studies have shown that hRev1 utilizes a protein template-directed mechanism to instruct dCTP incorporation through hydrogen bonding between cytosine and residue R357 of hRev1 (Figure 1) (*23*). To evaluate the roles of hydrogen bonding, base stacking, and base size during DNA synthesis, we have measured the catalytic efficiency of hRev1 incorporating two non-natural nucleotide analogues into D-G DNA (Figure 3A and Table 3). Both dPTP and dNITP lack the ability to form strong hydrogen bonds, possess greater base stacking energy, and are physically larger than dCTP (*37*). hRev1 can incorporate both analogues, although the incorporation efficiency decreases by 3500- and 11000-fold for dNITP and dPTP, respectively. Both analogues are incorporated with significantly reduced rates (at least 490-fold) and modestly weakened binding affinities (at least 7-fold). These data suggested that hydrogen bonding is not essential for catalysis, but it does enhance the rate and binding affinity for dCTP incorporation.

Kinetic Basis of Ribonucleotide Selection. The concentrations of cellular dNTP pools fluctuate during the cell cycle, and the levels are 10−200-fold lower than those of the ribonucleotide (rNTP) pools that remain relatively high and constant (*38*, *39*). Since hRev1 has been shown to be present outside of S phase (*28*), we have evaluated the sugar selectivity of hRev1 by measuring the substrate specificity constant for various CTP analogues (Figure 3B and Table 4). hRev1 discriminates between dCTP and rCTP by 280-fold, and this is mostly due to a 230-fold rate decrease. To improve our understanding of how size and orientation affect the degree of sugar selectivity, we have used araCTP (an anticancer drug that is a steric isomer of rCTP with the 2′-OH group pointed above the ribose ring), 2′-F-CTP (the 2′-F group is smaller than the 2′-OH group), GemCTP

(an anticancer drug with two fluorines at the 2′-position), and 2′-OCH_3-CTP (the 2′-OCH_3 group is larger than the 2′-OH group). The orientation and reduced size of the 2′-group are important factors because the efficiency of hRev1 incorporating araCTP and 2′-F-CTP was similar to that for dCTP. In contrast, the increased volume of the 2′-methoxy group enhanced the magnitude of discrimination to 6700. Surprisingly, most of the sugar selection was k_p-driven for hRev1. The one exception is for GemCTP where the K_d value increased by 13-fold.

DISCUSSION

Comparison of Base Substitution Fidelity. As a dCTP transferase, Rev1 is a DNA polymerase with an extremely low fidelity because of the preference to form dCTP·dN base pairs over canonical Watson−Crick base pairs dTTP·dA, dATP·dT, and dGTP·dC. Using pre-steady-state kinetic methods, we have established a base substitution fidelity from 10^0 to 10^{-5} for truncated hRev1 synthesizing undamaged DNA (Table 2). This fidelity range is similar to those of other human Y-family DNA polymerases (*40*) and a fidelity range from 10^0 to 10^{-4} that was estimated for full-length hRev1 under semi-steady-state kinetic conditions by Zhang et al. (*22*). In their studies, Zhang et al. used too much full-length hRev1 (14 fmol) in the reactions with 50 fmol of DNA and various dNTPs at 30 °C (*22*), possibly due to the lack of quantifiable reaction products during non-dCTP incorporations. Thus, their semi-steady-state kinetic parameters cannot be used to kinetically describe nucleotide incorporation catalyzed by hRev1. In this paper, we employed pre-steady-state kinetic methods to investigate the kinetic basis for nucleotide selection and enzyme fidelity for hRev1. Our kinetic data revealed that hRev1 discriminates at both the nucleotide binding (K_d) and incorporation (k_p) steps. Overall, hRev1 prefers the dCTP·dG base pair with a 20-fold tighter binding affinity and a 14-fold faster rate of incorporation (on average) with undamaged DNA relative to the other tested dNTP·dN base pair combinations (Table 2).

Pre-steady-state kinetic analyses have been conducted with a truncated form of yeast Rev1 (yRev1, 1−746) (*41*). In stark contrast, yRev1 selects incoming nucleotides mostly at the nucleotide binding step (K_d). The catalytic efficiency for the dCTP·dG base pair is 660-fold greater for the human enzyme, and this effect is governed by a ∼1900-fold faster rate of dCTP incorporation catalyzed by hRev1 at 37 °C (22.4 s^{-1}) versus yRev1 at 22 °C (0.012 s^{-1}), although hRev1 (2.2 μM) binds dCTP with a 3-fold weaker affinity than yRev1 (0.78 μM) (*41*). Interestingly, significant kinetic differences have been observed for human and yeast Polη at varying reaction temperatures, too (*42*). Thus, it is important to exercise caution when extending conclusions about DNA polymerase homologues derived from different organisms (*14*, *43*).

Effect of DNA Substrate on the Catalytic Efficiency of hRev1. Translesion DNA synthesis has been proposed to proceed through a polymerase-switching or gap-filling model (*44*). Also, Rev1 has been shown to be important during UV-induced postreplicative gap-filling processes that likely occur outside of S phase (*36*, *44*). Although the incorporation efficiency decreased by ∼7-fold from nongapped to gapped DNA, hRev1 is capable of accommodating a single-nucleotide gap DNA substrate despite lacking the signature helix−hairpin−helix (HhH) motif that Polβ and Polλ, two X-family DNA polymerases specialized for gap-filling DNA synthesis, use to bind the downstream strand. Moreover, the gap filling efficiency of 1.4 μM^{-1} s^{-1} for hRev1 is close or similar to the values measured for rat Polβ (6.6 μM^{-1} s^{-1}) and human Polλ (1.8 μM^{-1} s^{-1}) (Table 2) (*45*, *46*). More studies are needed to evaluate whether hRev1 plays a role in gap-filling DNA synthesis *in vivo*.

Kinetic Basis for Nucleotide Selection. Watson−Crick hydrogen bond formation between the template base and incoming dNTP has been shown to play an important role in nucleotide selection by many DNA polymerases, including T7 DNA polymerase (*47*). However, hRev1 does not use this DNA template-dependent mechanism to select incoming dNTPs. Instead, it uses the protein template-directed mechanism while the templating base dG is evicted from the active site by L358 so that it fits into a hydrophobic pocket surrounded by F525, K770, and H774 (Figure 1). To probe whether hydrogen bonds between cytosine and R357 are essential for catalysis by hRev1, we examined if hRev1 could incorporate dNITP and dPTP which are unable to form hydrogen bonds. Although the efficiency was reduced dramatically (Table 3), these non-natural nucleotide analogues were incorporated into DNA by hRev1. These results suggested that hydrogen bonds formed between the incoming dNTP and R357 are important, but not absolutely essential, for efficient nucleotide incorporation catalyzed by hRev1 and that an oversized nucleobase with strong base stacking energy can be accommodated. To improve our understanding of the role of hydrogen bonds, additional studies need to be performed using isosteric, non-hydrogen bonding dCTP analogues.

Previously, Howell et al. (*41*) proposed possible interactions (i.e., hydrogen bonds and base conformations) for the four dNTP·Arg combinations based on the X-ray crystal structures of yRev1·DNA·dCTP (*48*) and *Escherichia coli* MutM DNA glycosylase·DNA (*49*). Interestingly, the number of hydrogen bonds correlates with the substrate specificity of dNTP incorporation into DNA with dG as the template for both yRev1 and hRev1: dCTP (two hydrogen bonds) > dGTP (two hydrogen bonds if dGTP adopts a *syn* conformation) ≈ dTTP (one hydrogen bond) > dATP (zero hydrogen bonds) (*41*, *50*). However, the identity of the template base also contributes to catalytic efficiency since dCTP misincorporation is less efficient for hRev1 (Table 2). Thus, the optimal catalytic activity (k_p/K_d) of hRev1 depends on both substrates: an incoming dCTP and the template base dG.

Kinetic Basis for Ribonucleotide Exclusion. Most DNA polymerases prevent ribonucleotide incorporation via a steric clash between the 2′-OH group of an incoming rNTP and a protein backbone segment (*51*) or bulky side chain residue of the enzyme (*52*−*56*). This mechanism usually yields sugar selectivity values greater than 1000-fold (*51*, *52*, *54*−*57*). hRev1 discriminates between dCTP and rCTP by 280-fold, a value that is relatively low compared to those of other DNA polymerases (Table 4). Like other DNA polymerases, hRev1 possesses a putative steric gate residue F428, but its benzene ring almost parallels and stacks with the ribose ring (Figure 1) (*23*). Thus, it is unclear how hRev1 discriminates against rNTPs. In general, the kinetic basis for rNTP discrimination by most DNA polymerases occurs via weakened binding and slower incorporation of rNTPs. Using CTP analogues, we showed that the mechanism of ribonucleotide selection employed by hRev1 is influenced by both the size and orientation of the 2′-group (Table 4). With varying sizes of the 2′-substituent, the K_d values for 2′-F-CTP, rCTP, araCTP, and 2′-OCH_3-CTP were not affected significantly. This is probably due to the favorable hydrogen bonding interactions between residue R357 of hRev1 and the cytosine

base which compensated for the steric effect of the 2′-substituent. However, the binding of GemCTP to hRev1·D-G DNA was perturbed the most, with an affinity 13-fold lower than that of dCTP. The geminal difluoro group of GemCTP has more electronegativity than the deoxyribose of dCTP, and an embedded GemCMP residue in duplex DNA adopts a C3′-endo pucker (*58*). These may affect how GemCTP was positioned in the active site and how it interacted with R357 and F428 of hRev1, leading to the lower affinity. Interestingly, a similar conclusion has been drawn for the human mitochondrial DNA polymerase γ incorporating GemCTP (*59*). In comparison, Table 4 shows that the k_p variation is much larger than the K_d range for the CTP analogues. If the ribose 2′-substituent either is small (e.g., 2′-F in both 2′-F-CTP and GemCTP) or is oriented above the ribose ring (e.g., 2′-OH in araCTP), it has a small impact on the k_p value. Contrary to these trends, the k_p values for rCTP and 2′-OCH_3-CTP are 200−2000-fold lower than that of dCTP. Together, these results suggested that, inconsistent with the general kinetic trends observed with other DNA polymerases (see above), the steric clash of the 2′-OH group of the incoming rCTP with F428 of hRev1 mostly impacts the incorporation step (k_p) rather than the ground-state binding step (K_d). In addition to the major contribution of the templating base dG to the high dCTP incorporation efficiency (see the discussion above), our kinetic data further dissect the contribution of each chemical moiety to the high efficiency of dCTP incorporation catalyzed by hRev1: the ribose 2′-H of dCTP significantly contributes to the fast k_p, while the cytosine of dCTP contributes to the low K_d for dCTP binding. We are currently elucidating the kinetic mechanism of dCTP incorporation to mechanistically understand how these chemical moieties of dCTP influence its k_p and K_d.

ACKNOWLEDGMENT

We thank Dr. John-Stephen Taylor for providing dPTP and Dr. Kenji Kamiya for providing expression plasmid pBAD-REV1S.

REFERENCES

1. Burgers, P. M., Koonin, E. V., Bruford, E., Blanco, L., Burtis, K. C., Christman, M. F., Copeland, W. C., Friedberg, E. C., Hanaoka, F., Hinkle, D. C., Lawrence, C. W., Nakanishi, M., Ohmori, H., Prakash, L., Prakash, S., Reynaud, C. A., Sugino, A., Todo, T., Wang, Z., Weill, J. C., and Woodgate, R. (2001) Eukaryotic DNA polymerases: Proposal for a revised nomenclature. *J. Biol. Chem. 276*, 43487–43490.
2. Lin, W., Xin, H., Zhang, Y., Wu, X., Yuan, F., and Wang, Z. (1999) The human REV1 gene codes for a DNA template-dependent dCMP transferase. *Nucleic Acids Res. 27*, 4468–4475.
3. Yang, W., and Woodgate, R. (2007) What a difference a decade makes: Insights into translesion DNA synthesis. *Proc. Natl. Acad. Sci. U.S.A. 104*, 15591–15598.
4. Ross, A. L., Simpson, L. J., and Sale, J. E. (2005) Vertebrate DNA damage tolerance requires the C-terminus but not BRCT or transferase domains of REV1. *Nucleic Acids Res. 33*, 1280–1289.
5. Guo, C., Sonoda, E., Tang, T. S., Parker, J. L., Bielen, A. B., Takeda, S., Ulrich, H. D., and Friedberg, E. C. (2006) REV1 protein interacts with PCNA: Significance of the REV1 BRCT domain in vitro and in vivo. *Mol. Cell 23*, 265–271.
6. Guo, C., Tang, T. S., Bienko, M., Parker, J. L., Bielen, A. B., Sonoda, E., Takeda, S., Ulrich, H. D., Dikic, I., and Friedberg, E. C. (2006) Ubiquitin-binding motifs in REV1 protein are required for its role in the tolerance of DNA damage. *Mol. Cell. Biol. 26*, 8892–8900.
7. Wood, A., Garg, P., and Burgers, P. M. (2007) A ubiquitin-binding motif in the translesion DNA polymerase Rev1 mediates its essential functional interaction with ubiquitinated proliferating cell nuclear antigen in response to DNA damage. *J. Biol. Chem. 282*, 20256–20263.
8. Murakumo, Y., Ogura, Y., Ishii, H., Numata, S., Ichihara, M., Croce, C. M., Fishel, R., and Takahashi, M. (2001) Interactions in the error-prone postreplication repair proteins hREV1, hREV3, and hREV7. *J. Biol. Chem. 276*, 35644–35651.
9. Guo, C., Fischhaber, P. L., Luk-Paszyc, M. J., Masuda, Y., Zhou, J., Kamiya, K., Kisker, C., and Friedberg, E. C. (2003) Mouse Rev1 protein interacts with multiple DNA polymerases involved in translesion DNA synthesis. *EMBO J. 22*, 6621–6630.
10. Masuda, Y., Ohmae, M., Masuda, K., and Kamiya, K. (2003) Structure and enzymatic properties of a stable complex of the human REV1 and REV7 proteins. *J. Biol. Chem. 278*, 12356–12360.
11. Tissier, A., Kannouche, P., Reck, M. P., Lehmann, A. R., Fuchs, R. P. P., and Cordonnier, A. (2004) Co-localization in replication foci and interaction of human Y-family members, DNA polymerase pol η and REV1 protein. *DNA Repair 3*, 1503–1514.
12. Ohashi, E., Murakumo, Y., Kanjo, N., Akagi, J., Masutani, C., Hanaoka, F., and Ohmori, H. (2004) Interaction of hREV1 with three human Y-family DNA polymerases. *Genes Cells 9*, 523–531.
13. Yuasa, M. S., Masutani, C., Hirano, A., Cohn, M. A., Yamaizumi, M., Nakatani, Y., and Hanaoka, F. (2006) A human DNA polymerase η complex containing Rad18, Rad6 and Rev1: Proteomic analysis and targeting of the complex to the chromatin-bound fraction of cells undergoing replication fork arrest. *Genes Cells 11*, 731–744.
14. Kosarek, J. N., Woodruff, R. V., Rivera-Begeman, A., Guo, C., D'Souza, S., Koonin, E. V., Walker, G. C., and Friedberg, E. C. (2008) Comparative analysis of in vivo interactions between Rev1 protein and other Y-family DNA polymerases in animals and yeasts. *DNA Repair 7*, 439–451.
15. Ohashi, E., Hanafusa, T., Kamei, K., Song, I., Tomida, J., Hashimoto, H., Vaziri, C., and Ohmori, H. (2009) Identification of a novel REV1-interacting motif necessary for DNA polymerase κ function. *Genes Cells 14*, 101–111.
16. Kannouche, P., and Stary, A. (2003) Xeroderma pigmentosum variant and error-prone DNA polymerases. *Biochimie 85*, 1123–1132.
17. Friedberg, E. C., Lehmann, A. R., and Fuchs, R. P. (2005) Trading places: How do DNA polymerases switch during translesion DNA synthesis? *Mol. Cell 18*, 499–505.
18. Lehmann, A. R., Niimi, A., Ogi, T., Brown, S., Sabbioneda, S., Wing, J. F., Kannouche, P. L., and Green, C. M. (2007) Translesion synthesis: Y-family polymerases and the polymerase switch. *DNA Repair 6*, 891–899.
19. Masuda, Y., Takahashi, M., Tsunekuni, N., Minami, T., Sumii, M., Miyagawa, K., and Kamiya, K. (2001) Deoxycytidyl transferase activity of the human REV1 protein is closely associated with the conserved polymerase domain. *J. Biol. Chem. 276*, 15051–15058.
20. Masuda, Y., and Kamiya, K. (2002) Biochemical properties of the human REV1 protein. *FEBS Lett. 520*, 88–92.
21. Choi, J. Y., and Guengerich, F. P. (2008) Kinetic analysis of translesion synthesis opposite bulky N2- and O6-alkylguanine DNA adducts by human DNA polymerase REV1. *J. Biol. Chem. 283*, 23645–23655.
22. Zhang, Y., Wu, X., Rechkoblit, O., Geacintov, N. E., Taylor, J. S., and Wang, Z. (2002) Response of human REV1 to different DNA damage: Preferential dCMP insertion opposite the lesion. *Nucleic Acids Res. 30*, 1630–1638.
23. Swan, M. K., Johnson, R. E., Prakash, L., Prakash, S., and Aggarwal, A. K. (2009) Structure of the human Rev1-DNA-dNTP ternary complex. *J. Mol. Biol. 390*, 699–709.
24. Lawrence, C. W. (2002) Cellular roles of DNA polymerase ζ and Rev1 protein. *DNA Repair 1*, 425–435.
25. Clark, D. R., Zacharias, W., Panaitescu, L., and McGregor, W. G. (2003) Ribozyme-mediated REV1 inhibition reduces the frequency of UV-induced mutations in the human HPRT gene. *Nucleic Acids Res. 31*, 4981–4988.
26. Simpson, L. J., and Sale, J. E. (2003) Rev1 is essential for DNA damage tolerance and non-templated immunoglobulin gene mutation in a vertebrate cell line. *EMBO J. 22*, 1654–1664.
27. Murakumo, Y., Mizutani, S., Yamaguchi, M., Ichihara, M., and Takahashi, M. (2006) Analyses of ultraviolet-induced focus formation of hREV1 protein. *Genes Cells 11*, 193–205.
28. Akagi, J., Masutani, C., Kataoka, Y., Kan, T., Ohashi, E., Mori, T., Ohmori, H., and Hanaoka, F. (2009) Interaction with DNA polymerase η is required for nuclear accumulation of REV1 and suppression of spontaneous mutations in human cells. *DNA Repair 8*, 585–599.
29. Ross, A. L., and Sale, J. E. (2006) The catalytic activity of REV1 is employed during immunoglobulin gene diversification in DT40. *Mol. Immunol. 43*, 1587–1594.
30. Jansen, J. G., Langerak, P., Tsaalbi-Shtylik, A., van den Berk, P., Jacobs, H., and de Wind, N. (2006) Strand-biased defect in C/G

transversions in hypermutating immunoglobulin genes in Rev1-deficient mice. *J. Exp. Med. 203*, 319–323.
31. Masuda, Y., and Kamiya, K. (2006) Role of single-stranded DNA in targeting REV1 to primer termini. *J. Biol. Chem. 281*, 24314–24321.
32. Fiala, K. A., and Suo, Z. (2004) Pre-steady-state kinetic studies of the fidelity of *Sulfolobus solfataricus* P2 DNA polymerase IV. *Biochemistry 43*, 2106–2115.
33. Fiala, K. A., Abdel-Gawad, W., and Suo, Z. (2004) Pre-steady-state kinetic studies of the fidelity and mechanism of polymerization catalyzed by truncated human DNA polymerase λ. *Biochemistry 43*, 6751–6762.
34. Johnson, K. A. (1992) Transient-state kinetic analysis of enzyme reaction pathways. *Enzymes 20*, 1–61.
35. Tsai, Y. C., and Johnson, K. A. (2006) A new paradigm for DNA polymerase specificity. *Biochemistry 45*, 9675–9687.
36. Jansen, J. G., Tsaalbi-Shtylik, A., Hendriks, G., Gali, H., Hendel, A., Johansson, F., Erixon, K., Livneh, Z., Mullenders, L. H., Haracska, L., and de Wind, N. (2009) Separate domains of Rev1 mediate two modes of DNA damage bypass in mammalian cells. *Mol. Cell. Biol. 29*, 3113–3123.
37. Guckian, K. M., Schweitzer, B. A., Ren, R. X.-F., Sheils, C. J., Tahmassebi, D. C., and Kool, E. T. (2000) Factors contributing to aromatic stacking in water: Evaluation in the context of DNA. *J. Am. Chem. Soc. 122*, 2213–2222.
38. Kornberg, A., and Baker, T. A. (1992) DNA Replication, 2nd ed., W. H. Freeman, New York.
39. Traut, T. W. (1994) Physiological concentrations of purines and pyrimidines. *Mol. Cell. Biochem. 140*, 1–22.
40. McCulloch, S. D., and Kunkel, T. A. (2008) The fidelity of DNA synthesis by eukaryotic replicative and translesion synthesis polymerases. *Cell Res. 18*, 148–161.
41. Howell, C. A., Prakash, S., and Washington, M. T. (2007) Pre-steady-state kinetic studies of protein-template-directed nucleotide incorporation by the yeast Rev1 protein. *Biochemistry 46*, 13451–13459.
42. Washington, M. T., Johnson, R. E., Prakash, L., and Prakash, S. (2003) The mechanism of nucleotide incorporation by human DNA polymerase η differs from that of the yeast enzyme. *Mol. Cell. Biol. 23*, 8316–8322.
43. Poltoratsky, V., Horton, J. K., Prasad, R., and Wilson, S. H. (2005) REV1 mediated mutagenesis in base excision repair deficient mouse fibroblast. *DNA Repair 4*, 1182–1188.
44. Waters, L. S., Minesinger, B. K., Wiltrout, M. E., D'Souza, S., Woodruff, R. V., and Walker, G. C. (2009) Eukaryotic translesion polymerases and their roles and regulation in DNA damage tolerance. *Microbiol. Mol. Biol. Rev. 73*, 134–154.
45. Ahn, J., Kraynov, V. S., Zhong, X., Werneburg, B. G., and Tsai, M. D. (1998) DNA polymerase β: Effects of gapped DNA substrates on dNTP specificity, fidelity, processivity and conformational changes. *Biochem. J. 331* (Part 1), 79–87.
46. Fiala, K. A., Duym, W. W., Zhang, J., and Suo, Z. (2006) Up-regulation of the fidelity of human DNA polymerase λ by its non-enzymatic proline-rich domain. *J. Biol. Chem. 281*, 19038–19044.
47. Kool, E. T., and Sintim, H. O. (2006) The difluorotoluene debate: A decade later. *Chem. Commun.,* 3665–3675.
48. Nair, D. T., Johnson, R. E., Prakash, L., Prakash, S., and Aggarwal, A. K. (2005) Rev1 employs a novel mechanism of DNA synthesis using a protein template. *Science 309*, 2219–2222.
49. Fromme, J. C., and Verdine, G. L. (2002) Structural insights into lesion recognition and repair by the bacterial 8-oxoguanine DNA glycosylase MutM. *Nat. Struct. Biol. 9*, 544–552.
50. Haracska, L., Prakash, S., and Prakash, L. (2002) Yeast Rev1 protein is a G template-specific DNA polymerase. *J. Biol. Chem. 277*, 15546–15551.
51. Brown, J. A., Fiala, K. A., Fowler, J. D., Sherrer, S. M., Newmister, S. A., Duym, W. W., and Suo, Z. (2010) A Novel Mechanism of Sugar Selection Utilized by a Human X-Family DNA Polymerase. *J. Mol. Biol. 395*, 282–290.
52. Astatke, M., Ng, K., Grindley, N. D., and Joyce, C. M. (1998) A single side chain prevents *Escherichia coli* DNA polymerase I (Klenow fragment) from incorporating ribonucleotides. *Proc. Natl. Acad. Sci. U.S.A. 95*, 3402–3407.
53. Gardner, A. F., and Jack, W. E. (1999) Determinants of nucleotide sugar recognition in an archaeon DNA polymerase. *Nucleic Acids Res. 27*, 2545–2553.
54. Bonnin, A., Lazaro, J. M., Blanco, L., and Salas, M. (1999) A single tyrosine prevents insertion of ribonucleotides in the eukaryotic-type ϕ29 DNA polymerase. *J. Mol. Biol. 290*, 241–251.
55. Yang, G., Franklin, M., Li, J., Lin, T. C., and Konigsberg, W. (2002) A conserved Tyr residue is required for sugar selectivity in a Pol α DNA polymerase. *Biochemistry 41*, 10256–10261.
56. DeLucia, A. M., Grindley, N. D., and Joyce, C. M. (2003) An error-prone family Y DNA polymerase (DinB homolog from *Sulfolobus solfataricus*) uses a 'steric gate' residue for discrimination against ribonucleotides. *Nucleic Acids Res. 31*, 4129–4137.
57. Nick McElhinny, S. A., and Ramsden, D. A. (2003) Polymerase μ is a DNA-directed DNA/RNA polymerase. *Mol. Cell. Biol. 23*, 2309–2315.
58. Konerding, D., James, T. L., Trump, E., Soto, A. M., Marky, L. A., and Gmeiner, W. H. (2002) NMR structure of a gemcitabine-substituted model Okazaki fragment. *Biochemistry 41*, 839–846.
59. Fowler, J. D., Brown, J. A., Johnson, K. A., and Suo, Z. (2008) Kinetic investigation of the inhibitory effect of gemcitabine on DNA polymerization catalyzed by human mitochondrial DNA polymerase. *J. Biol. Chem. 283*, 15339–15348.